

Modelling of spray and combustion processes by using the Eulerian multiphase approach and detailed chemical kinetics

Zvonimir Petranović*¹, Wilfried Edelbauer², Milan Vujanović¹, Neven Duić¹

¹ University of Zagreb, Faculty of Mechanical Engineering and Naval Architecture, Croatia

² AVL List GmbH, Graz, Austria

Abstract

This research deals with computational modelling of non-reactive and reactive turbulent spray processes. The spray process is modelled using the Euler Eulerian multiphase approach together with a size-of-classes model where the discrete phase is considered as continuum and divided into sub-classes. The combustion process is modelled by taking into account chemical kinetics and solving homogeneous gas phase reactions. The combustion model is implemented into a commercial computational fluid dynamics code, and used in combination with previously validated spray sub-models. Several non-reactive cases are modelled by comparing the fuel spatial and temporal development to the available experimental data. The modelled results show excellent agreement for fuel penetration and mixture distributions. Furthermore, the developed method is validated by modelling reactive spray processes within constant volume vessel, and by comparing results to the Engine combustion network experimental data. The vessel conditions correspond well to diesel-like conditions in terms of gas residuals, pressure and temperature. Finally, the given results show a good agreement for the lift-off length and the ignition delay trends compared to the experimental data, but a slight discrepancy in the combustion process occurrence is observed.

Keywords: Eulerian, multiphase, spray, combustion, modelling

1. Introduction

As a result of better fuel-energy conversion compared to spark ignition engines [1], diesel engines have greater popularity on the transportation vehicle market. Their overall efficiency in terms of fuel consumption and pollutant emissions is highly dependent upon the fuel-air mixing which is strongly influenced by fuel atomisation and evaporation processes. The European Union promotes usage of different fuels for powering transportation vehicles [2]. Therefore, in order to remain the most used vehicle powering system, diesel engines must meet higher efficiency standards which can be achieved through their constant development [3]. Modern development methods combine experimental research with Computational Fluid Dynamics (CFD) tools which offer a cost-effective approach. The prerequisite for their reliable use is model accuracy achieved through the validation processes. In CFD modelling of diesel fuel combustion processes, the predictive spray model capabilities play the most important role [4]. Due to that fact, many researchers have invested their time in development of various spray modelling approaches.

In this research two modelling approaches for solving multiphase flows are mentioned: the Euler Eulerian (EE) and the Euler Lagrangian (EL) approach. The EL approach is the most widely used approach for engineering applications, but it suffers from several disadvantages as described in [5][6]. This approach is not able to adequately capture mass, momentum and energy inter-phase exchange in regions where the liquid void fraction dominates, i.e. the near nozzle region. To overcome the disadvantages of the EL approach, the EE modelling approach can be utilised. It provides a more reliable description of the physical processes in the nozzle vicinity. The EE approach represents a two-continuum flow description that can be further extended to a multi-continuum method dividing the dispersed phase into classes. The Eulerian conservation equations for mass, momentum and energy are solved for all classes, and the phase coupling is achieved through modelling of interphase exchange terms.

In Compression Ignition (CI) engines, the spray is formed due to high-pressure fuel injection through a small diameter nozzle. The liquid jet flows into the engine cylinder possessing a high momentum. This causes fuel jet disintegration into unstable ligaments and different sized droplets. In general, a spray can be divided into three different regimes: the dense, dilute and very dilute regime, depending on the concentration of the liquid phase. In the dense spray region, the liquid core disintegrates owing to turbulence induced forces and growing surface instabilities – this process is referred as the liquid jet primary atomisation. Such produced droplets are further influenced by relative inter-phase velocities and instabilities acting on the droplet surface. As a result, even smaller droplets are created – this process is called secondary atomisation process. It is essential to reliably model the spray process, since the CI engine combustion performance and emission formation are mainly influenced by the liquid fuel atomisation and the fuel-air mixing processes.

Reactive turbulent spray processes have been modelled by many authors employing various numerical approaches, such as eddy dissipation model, flamelet models, PDF method, detailed reaction mechanisms, etc. The use of the Eddy Dissipation Concept Model (EDC) was presented in [7], whilst combustion of diluted methanol and ethanol sprays was shown in [8][9][10]. The investigation to account for the influence of turbulence and nozzle geometry on spray combustion was performed in [11][12]. Furthermore, the influence of fuel injection timing on pollutant emission formation was shown in [13], whilst the prediction of NO and soot trends for various combustion parameters was shown in [14].

The modelling of reactive sprays by employing the EE approach was researched in the recent period, and a summary of relevant publications is briefly discussed. A diluted spray combustion process was modelled by employing the eddy breakup model, and results were presented in [15]. The PDF-Chemical equilibrium combustion model, without discretisation of the liquid phase, was presented in [16][17]. To avoid the difficulties of modelling the near nozzle region, a model for a

turbulent inflow boundary condition located downstream was presented in [18]. The diluted spray combustion was modelled by employing the tabulated chemistry approach in [19], whilst combustion of mono-dispersed sprays was researched in [20]. The authors highlighted the influence of the dispersed phase on the flame propagation. Furthermore, the importance of poly-dispersed sprays on the combustion process was shown in [21].

From the given literature review it can be concluded that the EE approach extended to a multi-continuum model has not been extensively tested on its ability to capture highly turbulent spray and combustion processes. The main objective of this research was to develop a new computational method capable to model the combustion process of poly-dispersed sprays. The presented method is suitable for modelling of multiphase reactive flows, and it can be utilized for modelling the processes occurring in dense spray region. The given results imply that the developed method is adequate for prediction of atomisation, collision, evaporation, and combustion processes.

The Engine Combustion Network (ECN) experimental data [22] of fuel injection with non-cavitating nozzle flow conditions were used for validation of the developed method. ECN is a worldwide group of institutions that perform both, experimental and numerical research. Their ultimate goal is to enrich the knowledge of spray and combustion processes at IC engine-relevant conditions. As a result of their work, a large set of experimental data was generated.

The paper is structured as follows: initially, the description of the developed method for modelling reactive sprays is presented in Section ‘Mathematical model’. The used ECN experimental data and the numerical setup are described in Section ‘Method plausibility, experimental data and numerical setup’. The comprehensive validation of the developed method is presented in Section ‘Results and discussion’. Next, the liquid and vapour penetration, mixture radial and spatial evolution, Lift-Off Length (LOL), Ignition Delay (ID), pressure rise, and Rate of Heat Release (ROHR) were investigated for different diesel-like conditions. Finally, the research conclusions are drawn in Section ‘Conclusions’.

2. Mathematical model

RANS based numerical simulations of the spray and combustion processes were performed. The EE size-of-classes model was used for modelling the highly turbulent spray behaviour. In this approach both the liquid and the gas phases are treated as interpenetrating continua defined by their volume fraction. The liquid phase is further divided into n classes according to the droplet diameter sorted in ascending manner. The first class is always defined as gas phase consisting of the contributing gas species. The classes from 2 to $n-1$ are the droplet classes, whilst the last class n is defined as a bulk liquid class with a diameter corresponding to the nozzle hole diameter. For each Eulerian class a separate set of conservation equations is solved, Equations (1), (2) and (3) [23]. The accuracy of the spray description depends on the number of classes. A higher number of droplet classes leads to a better resolution of the droplet size distribution function, but also to higher computational effort.

2.1. EE approach size-of-classes model

Employing the EE approach size-of-classes model a finite number of classes has to be defined together with the sources for the inter-phase exchange. The terms on the left-hand side of the conservation equations determine the property rate of change and the convective transport for class k . Terms Γ_{kl} , \mathbf{M}_{kl} and H_{kl} on the right-hand side are the modelled interfacial terms for mass, momentum and enthalpy exchange. Equation (4) represents the volume fraction compatibility condition that must be fulfilled in order to achieve property conservation.

$$\frac{\partial \alpha_k \rho_k}{\partial t} + \nabla \cdot (\alpha_k \rho_k \mathbf{v}_k) = \sum_{l=1, l \neq k}^n \Gamma_{kl} \quad (1)$$

$$\begin{aligned} \frac{\partial \alpha_k \rho_k \mathbf{v}_k}{\partial t} + \nabla \cdot (\alpha_k \rho_k \mathbf{v}_k \mathbf{v}_k) = & -\alpha_k \nabla p + \nabla \cdot \alpha_k (\boldsymbol{\tau}_k + \boldsymbol{\tau}'_k) + \alpha_k \rho_k \mathbf{f} + \\ & + \sum_{l=1, l \neq k}^n \mathbf{M}_{kl} + \mathbf{v}_{\text{int}} \sum_{l=1, l \neq k}^n \Gamma_{kl} \end{aligned} \quad (2)$$

$$\frac{\partial \alpha_k \rho_k h_k}{\partial t} + \nabla \cdot (\alpha_k \rho_k \mathbf{v}_k h_k) = \nabla \cdot \alpha_k (\mathbf{q}_k + \mathbf{q}_k^t) + \alpha_k \rho_k \mathbf{f} \cdot \mathbf{v}_k \quad (3)$$

$$+ \alpha_k \rho_k \theta_k + \alpha_k \boldsymbol{\tau}_k : \nabla \mathbf{v}_k + \alpha_k \frac{dp}{dt} + \sum_{l=1, l \neq k}^n \mathbf{H}_{kl} + h_{\text{int}} \sum_{l=1, l \neq k}^n \Gamma_{kl}$$

$$\sum_{k=1}^n \alpha_k = 1 \quad (4)$$

In Equations (1-4) term α stands for the class volume fraction, ρ is the class density, t denotes the time, \mathbf{v} is the class velocity vector, p is the pressure, $\boldsymbol{\tau}$ is the shear stress, $\boldsymbol{\tau}_k^t$ denotes the turbulent shear stress, \mathbf{f} is the body force vector, h is the specific enthalpy, whilst \mathbf{q} and \mathbf{q}_k^t are the heat flux and the turbulent heat flux terms, respectively.

The modelled sources are schematically shown in Figure 1. Term Γ_{kl} gets its contribution from the primary atomisation Γ_P , the secondary atomisation Γ_S , the droplet collision Γ_C and the droplet evaporation model Γ_E , as shown in Equation 5:

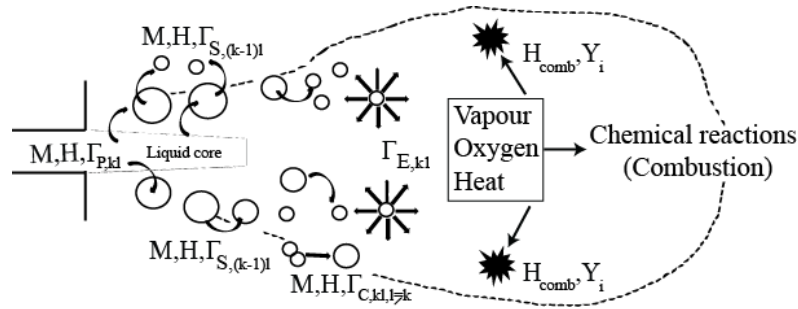


Figure 1 Schematic of the modelled sources

$$\Gamma_{kl} = \Gamma_{P,kl} + \Gamma_{S,kl} + \Gamma_{C,kl} + \Gamma_{E,kl} \quad (5)$$

A certain mass from the bulk liquid class n is transferred towards the droplet classes due to the primary breakup process. This process is modelled according to the “diesel core injection” model [24] which considers two independent mechanisms, aerodynamic surface wave growth and turbulence caused stresses. Index k in the modelled primary atomisation source term stands for the bulk liquid class, whilst index l stands for the target droplet class. To describe the droplet secondary atomisation process the common WAVE model is employed [25]. The source term arising from the secondary breakup process is used to model the mass transfer between droplet

classes indexed with k and l , where index k has the maximum value of $n-1$ and the minimum value of 2. This process is a one-way process which results in a mass shift from classes characterized with bigger diameter towards droplet classes with smaller diameter. It is a consequence of aerodynamic forces, acting on the droplet surface, and surface instabilities. Term $\Gamma_{C,kl}$ in Equation (5) stands for the mass source arising from droplet collisions. In this research, the collision process is modelled using the stochastic O'Rourke collision model [26] which was adopted for the EE approach [27]. The collision process is considered between different droplet classes with two possible outcomes, coalescence or no-collision outcome. The validation and parameterisation of the primary and secondary atomisation models have been presented in our previous work [28], where a detailed spray model validation is shown. The last term in Equation (5) stands for the mass shift due to the droplet evaporation process. It is modelled according to the Abramzon-Sirignano model [29], and the evaporated mass is transferred from all classes denoting from $2-n$ towards the gas phase.

During high-pressure fuel injection, the liquid jet disintegrates into relatively small droplets which tend to evaporate due to the elevated temperature conditions. The mass of the evaporated fuel enters the gas phase, and therefore, it is necessary to solve additional transport equations for all chemical species, as presented in Equation (6) [24]. Term Y_i on the left-hand side stands for the mass fraction of the i^{th} chemical species. The first term on the right-hand side is the diffusion term, where term D_{Y_i} is the species diffusion coefficient, Sc^t is the turbulent Schmidt number with the default value of 0.7, and μ_t^t is the turbulent viscosity. The term S_{Y_i} stands for the species mass source modelled by taking into account the species reaction rate and its molar mass.

$$\frac{\partial}{\partial t} \alpha_1 \rho_1 Y_i + \nabla \cdot \alpha_1 \rho_1 \mathbf{v}_1 Y_i = \nabla \cdot \left(\alpha_1 \left(\rho_1 D_{Y_i} + \frac{\mu_t^t}{Sc^t} \right) \nabla Y_i \right) + S_{Y_i} \quad (6)$$

2.2. Combustion modelling

The combustion process was modelled by using detailed chemistry kinetics. With such approach, a higher modelling accuracy is achieved, but compared to the commonly used combustion models the computational effort is increased. The source terms of the species transport equations and the gas phase enthalpy transport equation are determined by the reaction rates. To evaluate these reaction rates the internal chemistry interpreter of FIRE[®] was used [24]. It is based on the same theory which is implemented within the CHEMKIN library [30]. At the beginning of every time step in each computational cell a 0D reactor model is called. Based on the local flow field properties, additional terms in the transport equations are modelled, denoted by terms H_{comb} and Y_i . The expressions for enthalpy and species source terms are shown in Equation (7) and (8), where term Y_i stands for the mass fraction of the i^{th} species at the old (n) and the new ($n+1$) time step using the 0D reactor model. Term H_i stands for the heat of formation of species i whilst T_{ref} is the reference temperature.

$$S_{Y_i} = \frac{\rho^{n+1}Y_i^{n+1} - \rho^n Y_i^n}{\Delta t} \cdot V_{cell} \quad (7)$$

$$S_H = \sum_{i=1}^{K_{gas}} S_{Y_i} H_i \Big|_{T_{ref}} \frac{1}{w_i} \quad (8)$$

The exact chemistry of diesel fuels is hardly known and therefore a surrogate fuel mechanisms are commonly used. In this research, for modelling the n-heptane combustion process, the skeletal chemistry mechanism [31] covering 68 species and 283 chemical reactions is used. For modelling the n-dodecane combustion process another chemistry mechanism accounting for 106 chemical species and 420 chemical reactions is employed [32].

3. Method plausibility, experimental data and numerical setup

3.1. Method plausibility

The plausibility tests were performed by modelling the combustion process in a cuboid shaped constant volume reactor discretized with 2050 hexahedral control volumes. The domain boundary

surfaces were defined as constant temperature impermeable wall boundary condition. The domain was filled with a gas mixture (99.95% *vol.*) consisting of 24% O₂ and 76% N₂ (*mass*), whilst the rest of the volume was occupied by n-heptane fuel in liquid form. The initial gas temperature and pressure conditions were set to 1200 K and 2 MPa respectively, the fuel temperature was initialised with 323 K, and a quiescent environment was assumed. For the plausibility tests three Eulerian classes were defined, one for the gas phase and two droplet classes with diameters equal to 10 and 20 μm . The Abramzon-Sirignano evaporation model was used to model the droplet evaporation process. It should be mentioned that the exact evaporation rate, species concentration or temperature values were not of primary interest in this part of research. Instead, the overall system behaviour was observed.

The fuel droplets initialised within the reactor domain are subject to evaporation due to the elevated temperature conditions within the reactor. The concentration of fuel vapour rises according to the rules of the evaporation model and the reactor mean temperature decreases, as seen in Figure 2. The vaporised fuel reacts with the surrounding oxygen leading to a rapid heat release, temperature increase and production/destruction of certain species. When the reactant species are consumed the combustion process stops, the gas temperature reaches a “stationary” value, and the heat release from the chemical reactions is finished. The plausibility tests confirmed the correct implementation and the reasonable physical behaviour of the developed method.

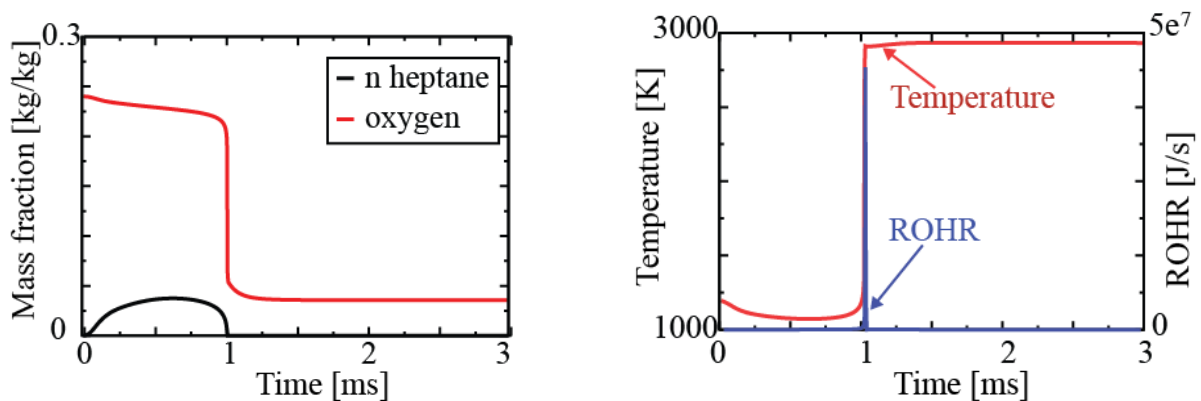


Figure 2 Plausibility test results

3.2. Experimental data and numerical set-up

For the method validation, several test cases from ECN web database [22] were modelled. The modelled Constant Volume Vessel (CVV) is made in cubical shape and has the characteristic dimensions of 108 mm. At the initial stage, the CVV was filled with a combustible gas mixture, and ignited with spark plugs placed on the vessel walls. Through the premixed combustion, the desired conditions in terms of temperature, pressure and Exhaust Gas Residuals (EGR) were achieved. These conditions are used as initial conditions in our modelling work. Next, the liquid fuel was injected with approximately 150 MPa pressure through a SAC type [33] injector located in the centre of a certain vessel wall. For the n-dodecane fuel injection, a nozzle with 84 μm hole diameter, the discharge coefficient of $C_d=0.9/0.89$ (0% $\text{O}_2/15\% \text{O}_2$), and the area contraction coefficient $C_a=0.98$ (all cases) was used. For the n-heptane injection cases, a 100 μm nozzle hole characterized with $C_d=0.8$ and $C_a=0.86$ was used. The modelled spray cases are described in Table 1.

Case	Fuel temp. [K]	CVV temp. [K]	CVV pressure [MPa]	Mixture composition [% vol]	Injection duration [ms]
n-heptane_0%O ₂	373	1000	4.33	3.77 H ₂ O,	6.8
n-dodecane_900K_0%O ₂		900	6.05	6.52 CO ₂ ,	
n-dodecane_1100K_0%O ₂	373	1100	4.96	89.71 N ₂ , 0 O₂	6
n-heptane_10%O ₂			4.28	3.67 H ₂ O, 6.32 CO ₂ , 80.01 N ₂ , 10 O₂	6.9
n-heptane_15%O ₂	373	1000	4.25	3.62 H ₂ O, 6.23 CO ₂ , 75.15 N ₂ , 15 O₂	6.8
n-heptane_21%O ₂			4.21	3.56 H ₂ O, 6.11 CO ₂ , 69.33 N ₂ , 21 O₂	6.8
n-dodecane_15%O ₂	363	1200	7.94	3.62 H ₂ O, 6.23 CO ₂ , 75.15 N ₂ , 15 O₂	6.1

Table 1 Initial conditions for modelled spray cases

In the first column of Table 1, the individual case titles are given. For the n-heptane spray modelling a computational mesh consisting of 11000 control volumes was used, whilst for the n-dodecane spray, a mesh with 8900 volumes was employed. The difference in the mesh size results from different nozzle-hole diameters. Both meshes were designed two-dimensional (2D) and axisymmetric, extending from 0 to 108 mm in axial direction and from 0 to 54 mm in radial direction. By using 2D computational meshes the computational time was significantly reduced. It is known that cavitation, nozzle geometry, and the motion of the injector needle have a direct impact on the spray development. In this research the normal velocity boundary condition calculated from the measured rate of the injection curve was applied. The influence of the inhomogeneous velocity distribution at the nozzle orifice and the influence of cavitation effects have been neglected. This is reasonable since the fuel injector was designed to suppress the cavitation process. The turbulence generated within the injector was taken into account by defining the mean k and ϵ values on the fuel inlet selection, where k stands for the turbulent kinetic energy and ϵ stands for the turbulent dissipation rate. For both meshes the nozzle inlet hole was refined with 5 faces over the nozzle radius, which yielded a smallest cell size of 10 μm for the n-heptane cases. The symmetry boundary condition was applied on the lateral surfaces, and the meshes were refined towards the spray inlet and the spray axis. The CVV and nozzle walls were defined as non-permeable wall boundary conditions with constant temperature, as recorded in the experimental research. In Figure 3 the boundaries for the n-heptane sprays are shown, and the same methodology was applied for the n-dodecane spray modelling.

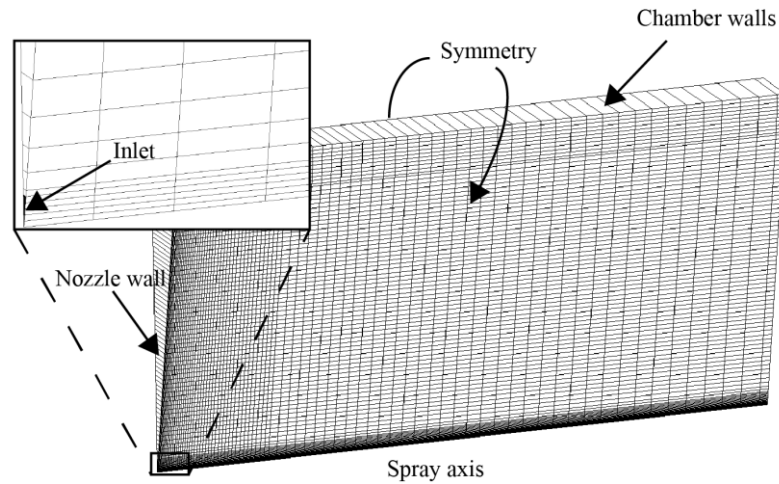


Figure 3 Computational domain for n-heptane spray modelling

Seven Eulerian classes were defined for modelling cases in the validation process - one for the gas phase and six classes for the liquid phase. The liquid phase was sorted into five droplet and one bulk liquid classes. The classes were defined with diameters of 1.5, 5, 10, 15, and 40 μm , whilst a diameter of 100 μm was assigned to the n-heptane bulk liquid class (84 μm for n-dodecane). For the turbulence, energy and volume fraction transport equations the first order upwind differencing scheme (UDS) was applied, whilst for the continuity equation the central differencing scheme (CDS) was employed. For the momentum equation a combination of CDS and UDS was proposed by introducing a blending factor of 0.5 [24][28]. The turbulence was modelled by using the advanced $k\zeta f$ - turbulence model [34][28]. The convergence of the solution was achieved when the normalized momentum, pressure and volume fraction residuals reached a value lower than $2 \cdot 10^{-4}$, and 10^{-4} for the energy residual. The pressure-velocity coupling was performed by using the SIMPLE algorithm. The time discretization level was varied over simulation time, where the maximum time step size was limited with the reaction rates of the used mechanisms. At the beginning of the injection process the time-step size was set to $5 \cdot 10^{-8}$ s and it was increased to a maximum value of 10^{-6} s. In this research, for modelling 1 ms of n-heptane spray and combustion processes on the computational mesh with 11000 control volumes, the simulation time was

approximately 3 hours (10 Intel® Xeon® CPU E5-2670 v3 @ 2.30GHz). All simulations were performed with the CFD software AVL FIRE®.

4. Results and Discussion

4.1. Non-reactive spray modelling

In order to tune the spray sub-model coefficients several non-reactive spray processes were modelled. For reliable modelling of IC engines combustion process, it is important to correctly describe the spray temporal and spatial development. In this research, the fuel penetration and mixing process were compared to the available experimental data, where the fuel penetration was defined through the spray mass threshold values [22]. The liquid penetration was defined as the furthest distance of the liquid phase where the spray mass accounted 90% of total liquid mass (a threshold value of 95% was defined for the gas phase).

4.1.1. N-heptane fuel injection

The comparison of modelled and measured data [35][36] for the fuel penetration is shown on the left-hand side of Figure 4, where a good agreement can be observed. The spray tip penetration curve is over-predicted in the initial stage, but at developed spray state it is correctly described. The reason for this error is most probably addressed to the primary breakup model. This model is developed and validated for fully developed spray and nozzle flow conditions, where high injection velocities occur. During the opening phase of the injector needle, the injection velocity and the turbulence are low. Consequently, the primary break-up could be under-estimated leading to droplets with large diameter, and over-predicted spray tip penetration during the initial stage of injection. Furthermore, a slightly underestimated vapour penetration at later stages can be addressed to the undersized droplet population as a result of the used spray sub-model coefficients. The liquid fuel starts to disintegrate into smaller droplets and ligaments – this effect is caused by the high liquid momentum arising from the injector/CVV pressure differences. Such created droplets tend to evaporate due to elevated temperature conditions, and the fuel vapour penetrates

into the vessel together with the spray jet. After the liquid jet has reached the developed state, the vapour cloud penetrates further into the domain. On the right-hand side in Figure 4 the radial mixture fraction profiles at the developed state (2.5 ms after SOI) are shown for four axial locations. The experimental data [37][38] are shown with different symbols whilst different continuous line styles are used to present the modelled data. The liquid fuel is injected along the spray axis, and owing to turbulent dispersion forces, the created droplets move in radial direction forming a conically shaped spray cloud. The droplet radial movement causes the spray angle and is responsible for the reduced fuel jet penetration. Additionally, it may influence the LOL in modelling of the reactive sprays. In the nozzle vicinity (approximately 20 mm in axial direction) the liquid jet is more concentrated in the spray axis region whilst far downstream a wider mixture distribution can be observed (40-50 mm).

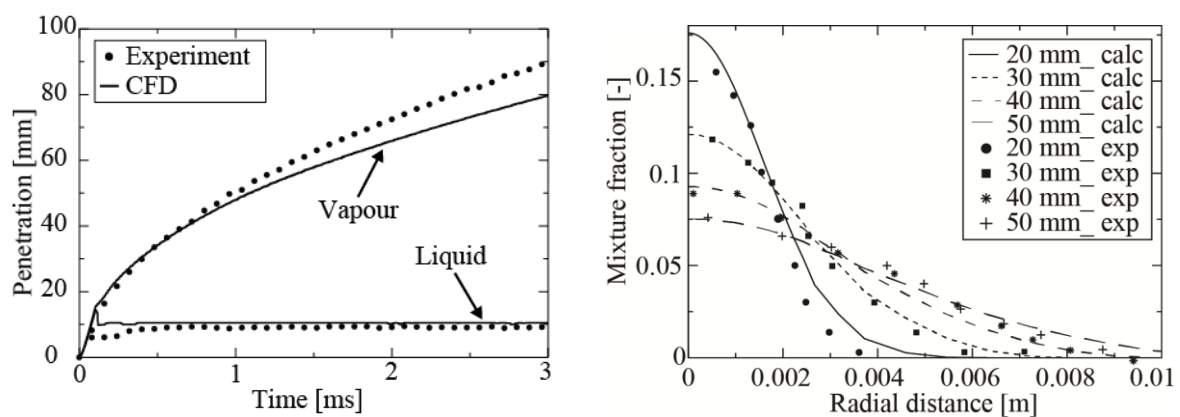


Figure 4 N-heptane_0%O₂: liquid and vapour penetration (left), mixture radial distribution (right)

The experimental images of the gas mixing process are averaged and compared to the modelled results, as shown in Figure 5. The deviation of the mean values from the experimental research are shown, and a 95% confidence interval was achieved. The given uncertainties are relatively high because only 30-40 images were taken during the experimental research. The upper group of four figures represents the comparison of the modelled results at 0.49 ms, whilst the lower group shows the penetration results for 1.13 ms after SOI [22][37][39]. The data in Figure 5 are shown for an

area extending from -14.2 to 14.2 mm in radial direction, and from 16.4 to 55.8 mm in axial direction.

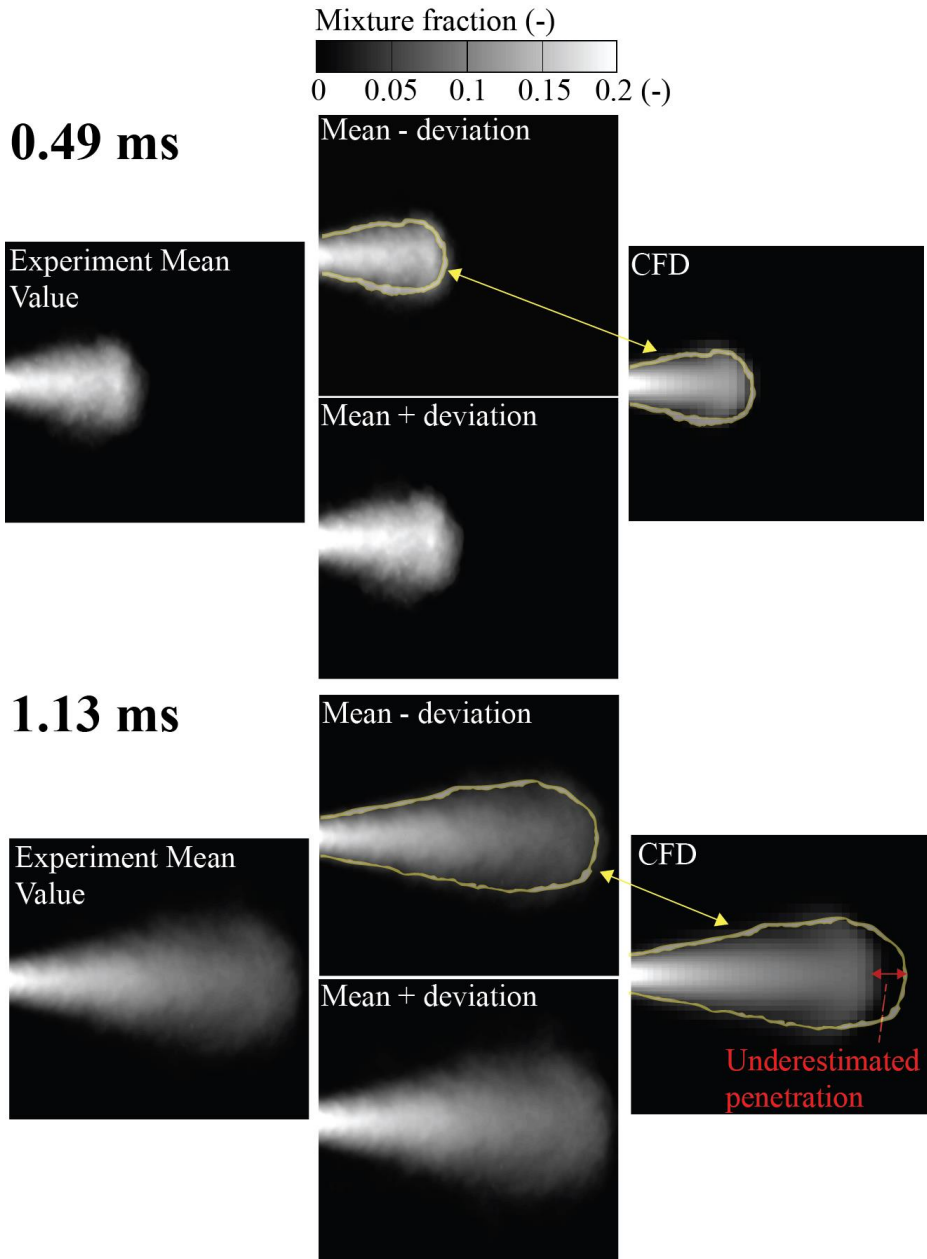


Figure 5 Mixture field comparison for case n-heptane_0%O₂

The modelled vapour cloud penetration is in good agreement with the experimental data at the early stage of injection, as it is visible by comparing the yellow contour extracted from the averaged experimental images. In the later stages, a slight underestimation of the mixture penetration is noticeable, which corresponds well to the penetration results shown in Figure 4. The underestimated vapour penetration may be addressed to the overrated atomisation process as a

result of the used spray sub-model parameters. With too intensive break-up many small droplets are created which cause too strong gas entrainment, and this leads consequently to smaller vapour penetrations. A further reason could be an overestimation of the turbulent viscosity from the applied eddy viscosity model, which causes also overestimated gas entrainment. In general, dispersed droplets or particles damp the turbulent fluctuations in the carrier gas. This effect was not modelled in the presented study.

The comparison of modelled and ensemble-averaged mean mixture temperature fields computed by using adiabatic mixing relationships for three different time steps is shown in Figure 6. A low temperature caused by the injected liquid fuel is noticeable in the region near the injection axis, whilst a higher temperature is visible at the periphery of the spray cloud. At later stages, higher temperatures are noticeable due to the heat transferred from the surrounding gas mixture. It is important to mention that the available experimental data are recorded from lateral positions, and therefore they represent the spray surface, whilst the modelled results are shown for the spray middle cross section.

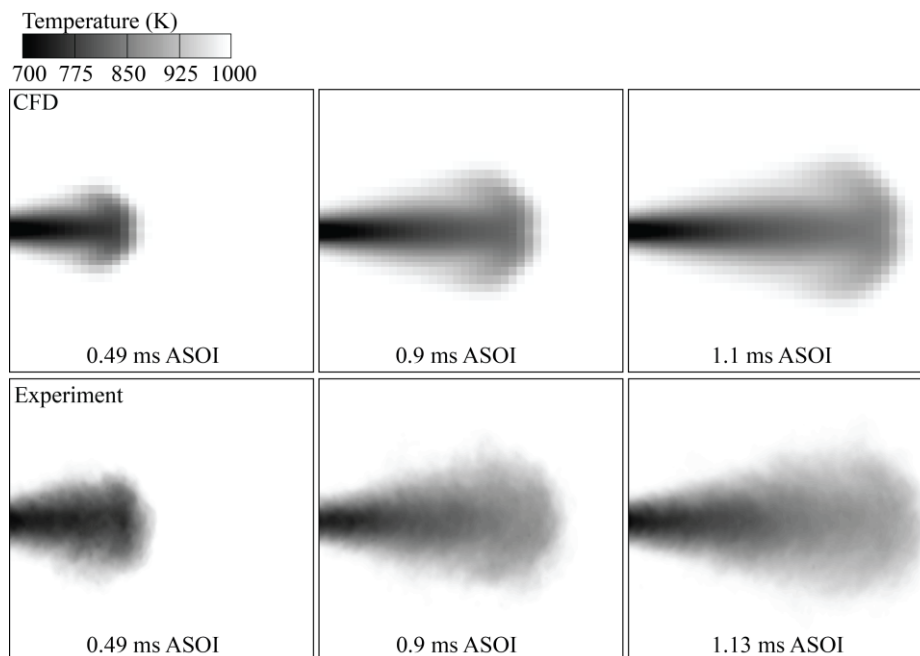


Figure 6 Averaged temperature field for case n-heptane_0%O₂

4.1.2. N-dodecane fuel injection

For further validation of the developed method, the non-reactive n-dodecane spray process was modelled. In Figure 7 the liquid and vapour fuel penetrations curves are shown for two spray cases, where a good agreement to the experimental data is visible. However, in modelling case n-dodecane_1100K_0%O₂ at later stages the vapour penetration is slightly underestimated. The reason for such behaviour, also noticed in modelling of the n-heptane case, may be addressed to the overestimated breakup mechanism, and consequently to the overrated dispersion of the vapour fuel in the radial direction. In addition, it should be mentioned that all spray sub-model parameters were chosen by modelling the injection of n-heptane fuel (case n-heptane_0%O₂) and used in all presented modelling cases.

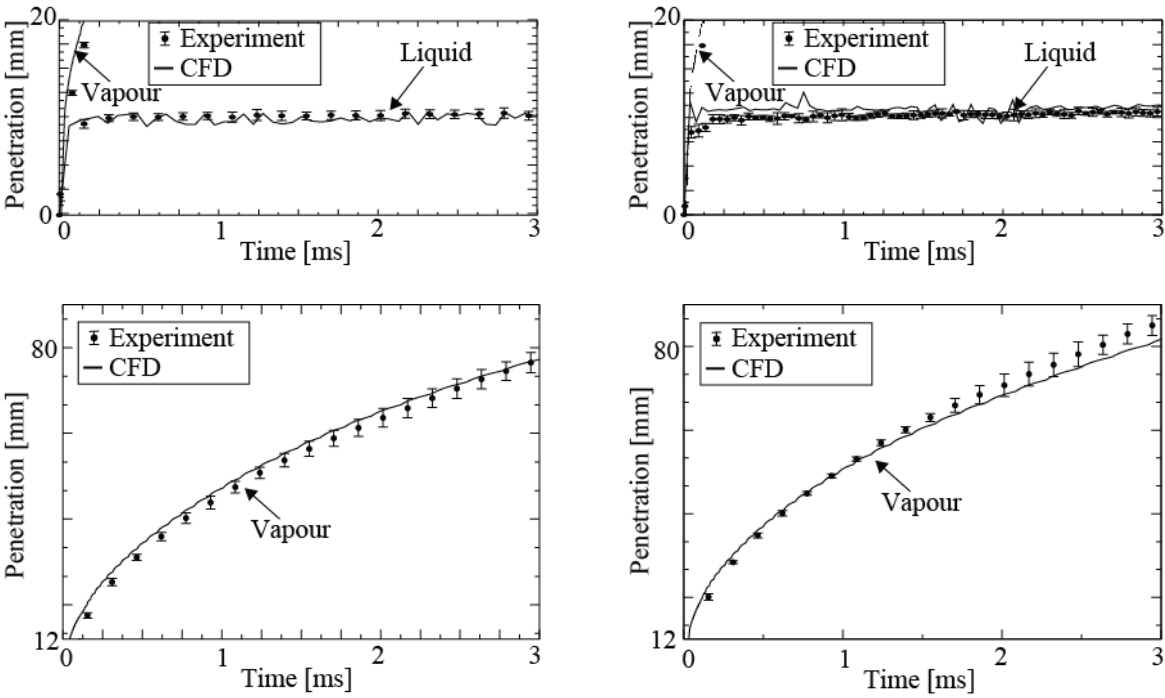


Figure 7 Spray penetration: n-dodecane_900K_0%O₂ (left) and n-dodecane_1100K_0%O₂ (right)

Mie-scattered light images were acquired during the spray quasi-steady period [40][41]. The first row in Figure 8 shows a comparison of the mixture fraction radial distribution at developed spray state for the two spray cases. The modelled results for case n-dodecane_1100K_0%O₂ show a higher mixture concentration in comparison to case n-dodecane_900K_0%O₂ which can be

addressed to the lower CVV pressure and the higher initial temperature of the gas mixture. In both cases, the vapour mixture is concentrated near the injection axis. The spray spreading is visible in the radial profiles at 45 mm, and it is more pronounced for case n-dodecane_1100K_0%O₂ which can be addressed to the lower CVV pressure. Overall, the presented results correspond well to the measured data for all monitoring locations except for 45 mm shown on the right-hand side where a slight underestimation of the radial distribution is visible. This difference may be a consequence of the chosen spray sub-models parameter set that was defined observing the n-heptane case (n-heptane_0%O₂). The second row in Figure 8 shows a comparison of the axial mixture distribution at developed spray state. The modelled results are shown in spray direction starting from the injection point up to 60 mm downstream. At the axial distance of approximately 10 mm the vaporisation rate is more pronounced for case n-dodecane_1100K_0%O₂ due to the higher CVV temperature condition. The mixture fraction decrease in axial direction can be addressed to the spray radial movement and causing a mass shift to the spray periphery.

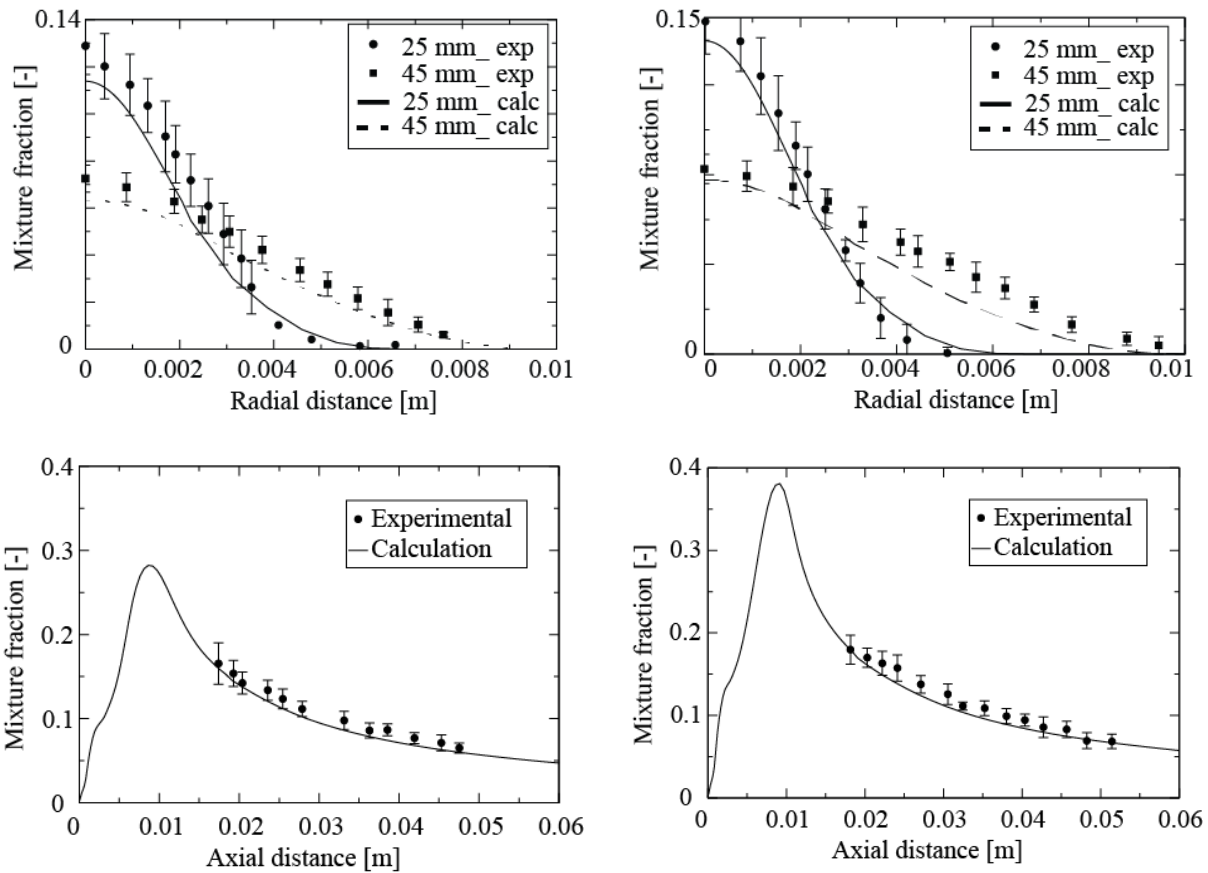


Figure 8 Mixture distribution; n-dodecane_900K_0%O₂ (left) and n-dodecane_1100K_0%O₂ (right)

The experimental images are averaged [22] for case n-dodecane_1100K_0%O₂ and compared to the modelled results, as shown in Figure 9. The images were recorded at spray developed state where the viewing area extends from 14.4 mm to 14.1 mm in radial direction, and from 17.8 mm to 51.6 mm in axial direction. On the left-hand side in Figure 9 a transport of vaporised fuel in radial direction is noticeable. This is the result of gas entrainment and turbulent forces acting on the fuel droplets. The upper figure shows a good comparison to the experimental data where the modelled results are placed within the measurement error boundaries. The comparison of temperature fields shows a slightly overestimated gas mixture temperature which is addressed to the underestimated modelled liquid fuel penetration. This may be a result, either of the slightly underestimated evaporation, or of the strong gas entrainment in the droplet covering area.

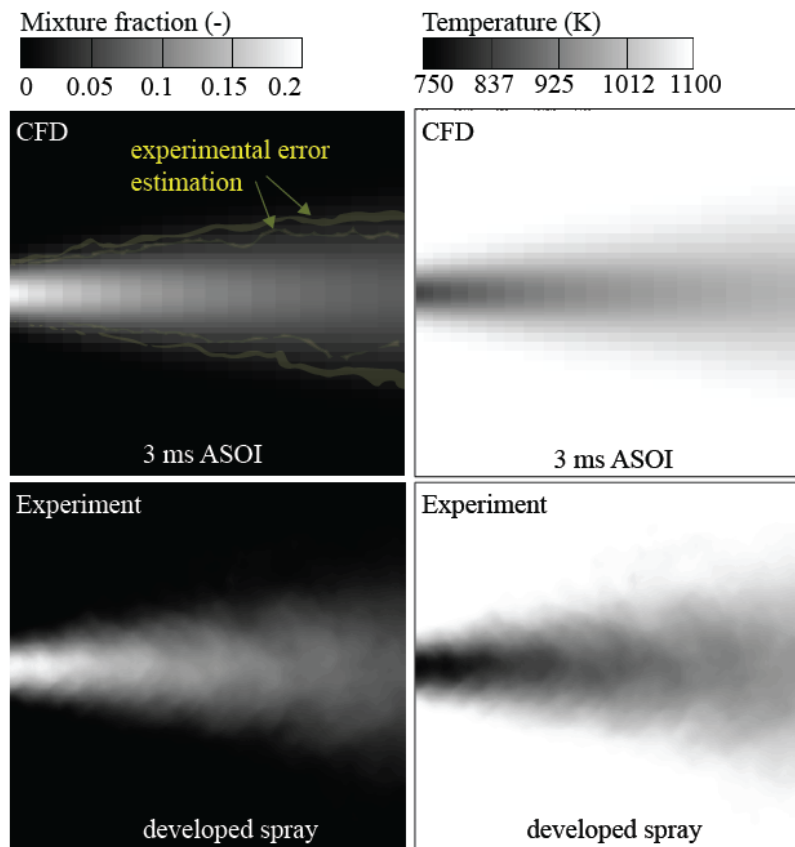


Figure 9 Averaged mixture (left) and temperature field (right) for case n-dodecane_1100K_0%O₂

4.2. Reactive spray simulations

Based on the calibrated spray sub-model parameters, the combustion process is modelled for different oxygen concentrations, fuels, nozzle geometries and CVV initial conditions. The validation of the developed method was performed by comparing the LOL, ignition delay (ID) and pressure rise to the available experimental data. The LOL is defined as the smallest distance from the injector where a temperature of 1600 K is recorded, and for some cases as a certain threshold value of the OH species concentration. The ID is defined as time after SOI when the ROHR has the maximum positive gradient.

4.2.1. N-heptane fuel injection into reactive environment

In this subsection, the modelling results for three reactive n-heptane spray cases are discussed. The main difference between the chosen cases is the initialized oxygen concentration at start of injection, as shown in Table 1. On the left-hand side of Figure 10, the comparison of modelled and measured LOL data is shown. Due to the mixing of evaporated fuel and hot environment, the vapour temperature increases and the combustion process occurs. This leads to a rapid temperature rise, and production of chemical species that further react following the rules of the used chemistry mechanism. In general, the comparison to experimental data shows a good agreement, but an underestimation of the LOL can be observed. This may be a consequence of slightly overrated atomisation process, uncertainties in the CVV initial conditions or of the used chemistry mechanism. When the atomisation of the liquid phase is overestimated, the spray Sauter mean diameter is smaller which influences the evaporation rate and the fuel-air mixing. Such behaviour will result in shorter LOL, which was expected based on presented modelling results of the non-reactive sprays. However, the overall LOL trend is correctly described, where a higher oxygen concentrations lead to shorter LOL, which corresponds well to the experimental data. The ID is

shown on the right-hand side in Figure 10, where the given results show a good agreement to the experimental data with slightly overestimated values for spray cases characterized with 15% and 21% oxygen concentration. The developed method and defined numerical setup reflect the physically correct behaviour, where the earlier occurrence of the combustion process can be addressed to the higher oxygen concentration.

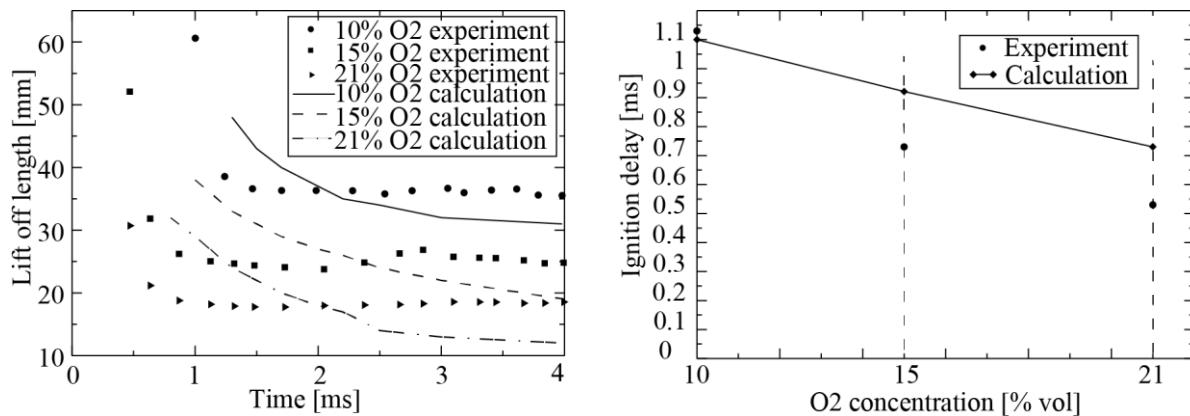


Figure 10 Lift-off length (left) and ignition delay time (right) for reactive n-heptane modelling cases

4.2.2. N-dodecane fuel injection into reactive environment

In this part of research the developed method was employed for modelling reactive spray processes where liquid n-dodecane fuel was injected into the pressurized CVV. The main differences compared to the modelled n-heptane spray cases are the injector design and the CVV initial conditions, as shown in Table 1. In Figure 11 the comparison of modelled and measured vapour penetration data is shown. Initially, the modelled vaporised fuel follows the measured penetration curve. At approximately 20 mm in axial direction and 0.35 ms after SOI the fuel vapour is completely consumed. At this point another species must be tracked to record the vapour cloud development. For that reason, the OH radical species was tracked. In Figure 11 black stars represent the modelled OH radical penetration for three different time frames (1, 2 and 3 ms after SOI), and a very good agreement to the experimental data can be observed.

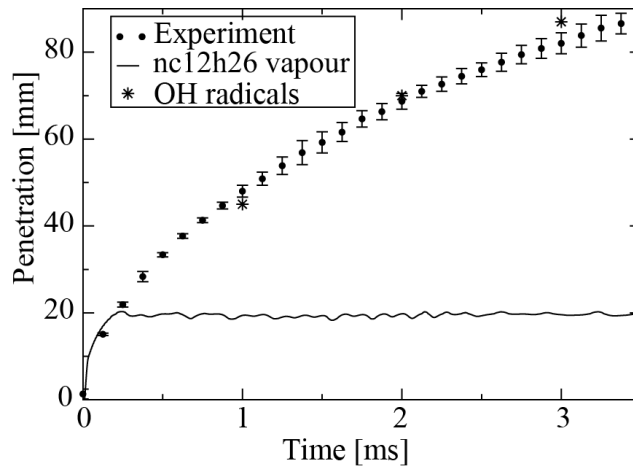


Figure 11 Vapour penetration (left) for case n-dodecane_15%O₂

The modelled LOL for the n-dodecane spray case is 10, 8 and 7 mm at 0.3, 0.5 ms and at the developed state, respectively. This corresponds well to the experimentally measured LOL in the developed state (7.6 mm). However, the modelled ID time is too long, since the combustion process is initially recorded at 0.2 ms after SOI, while the measured value is 0.11 ms. Such behaviour was expected based on our previous observations of non-reactive spray modelling and it can be explained by the same conclusions.

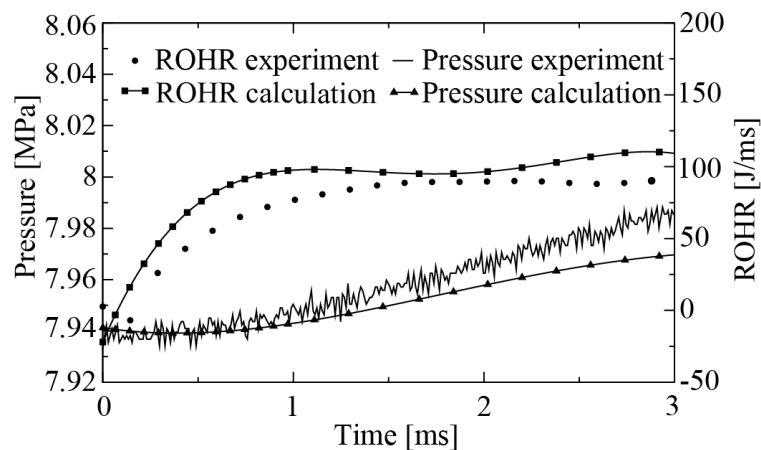


Figure 12 Comparison of combustion process for n-dodecane_15%O₂

Figure 12 shows the pressure rise where an almost linear trend is noticeable with a slight inclination at 0.2 ms after SOI. On the right axis the modelled ROHR is compared to the experimental data. The oscillatory behaviour of the modelled ROHR was averaged for better visibility, and a good comparison to the experimental data can be observed. The ROHR rapidly

increases during the initial stage of the combustion process (0.2 ms after SOI) until the flame reaches the fully developed state (around 1 ms after SOI).

5. Conclusion

The aim of this paper was to demonstrate a new method for computational modelling of mixture formation in non-reactive and reactive turbulent flows. This method combines the EE size-of-classes model together with the detailed chemistry kinetics. To check the method plausibility a reactor case was modelled, and a reasonable behaviour of the developed method is shown.

For method validation, several spray cases with different combustion parameters such as CVV initial conditions, injected mass, fuel type, etc. were modelled. Initially, the spray model coefficients were adjusted by modelling the non-reactive spray process. The same coefficients are later used for the reactive spray modelling. In the result analysis, the mixture distribution and fuel penetration were compared to available experimental data. The method successfully captured the influence of the nozzle diameter, fuel inlet conditions and CVV thermodynamic state on the overall spray development.

Additionally, several reactive spray cases were modelled and a good behaviour of the developed method was observed. The increase of ambient oxygen resulted in decrease of LOL and ID values, which corresponds well to the experimental observations. A slight underestimation of LOL and an overestimation of ID values was noticed, which can be improved through slight parameterization of the sub-model coefficients. However, the overall spray characteristics, global LOL and ID trends were described correctly. Also, the ROHR and pressure change due to the combustion process were found to be in good agreement to the available experimental data.

Based on the performed research it can be stated that the use of the developed method is reasonable for modelling of non-reactive liquid fuel injection. Furthermore, the presented method can be used for modelling of reactive sprays by employing detailed chemistry kinetics. However, a slight parameterization of the spray sub-model coefficients and research of the chemistry mechanisms is

recommended. The presented method provides a reliable description of the spray process in the dense spray region which makes it useful for modelling the processes in the near nozzle region. The computational effort depends on the number of Eulerian classes, the domain discretisation level and the applied chemistry mechanism.

Acknowledgments

The authors wish to thank AVL List GmbH, Graz, Austria for financing and opportunity to work on the research project. Authors would also wish to thank the CFD development group at AVL-AST, Graz, Austria, for their support and technical discussions during the model development. Finally, the authors would like to thank the Engine Combustion Network for providing valuable experimental data and simulation recommendations.

References

- [1]Katrašnik T. Hybridization of powertrain and downsizing of IC engine – A way to reduce fuel consumption and pollutant emissions – Part 1. *Energy Convers Manag* 2007;48:1411–23. doi:10.1016/j.enconman.2006.12.004.
- [2]Niemisto J, Saavalainen P, Pongracz E, Keiski RL. Biobutanol as a Potential Sustainable Biofuel - Assessment of Lignocellulosic and Waste-based Feedstocks. *J Sustain Dev Energy, Water Environ Syst* n.d.;1:58–77.
- [3]Kozarac D, Vuilleumier D, Saxena S, Dibble RW. Analysis of benefits of using internal exhaust gas recirculation in biogas-fueled HCCI engines. *Energy Convers Manag* 2014;87:1186–94. doi:10.1016/j.enconman.2014.04.085.
- [4]Fu-shui L, Lei Z, Bai-gang S, Zhi-jie L, Schock HJ. Validation and modification of WAVE spray model for diesel combustion simulation. *Fuel* 2008;87:3420–7. doi:10.1016/j.fuel.2008.05.001.
- [5]IYER V, ABRAHAM J. Penetration and Dispersion of Transient Gas Jets and Sprays. *Combust Sci Technol* 1997;130:315–34. doi:10.1080/00102209708935747.
- [6]Hallmann M, Scheurlen M, Wittig S. Computation of Turbulent Evaporating Sprays: Eulerian Versus Lagrangian Approach. *J Eng Gas Turbines Power* 1995;117:112. doi:10.1115/1.2812758.
- [7]Collazo J, Porteiro J, Patiño D, Miguez JL, Granada E, Moran J. Simulation and experimental validation of a methanol burner. *Fuel* 2009;88:326–34. doi:10.1016/j.fuel.2008.09.003.
- [8]Gutheil E. Numerical investigation of the ignition of dilute fuel sprays including detailed chemistry. *Combust Flame* 1993;93:239–54. doi:10.1016/0010-2180(93)90106-D.
- [9]Ge H-W, Gutheil E. Simulation of a turbulent spray flame using coupled PDF gas phase and spray flamelet modeling. *Combust Flame* 2008;153:173–85. doi:10.1016/j.combustflame.2007.10.019.

- [10] Düwel I, Ge H-W, Kronemayer H, Dibble R, Gutheil E, Schulz C, et al. Experimental and numerical characterization of a turbulent spray flame. *Proc Combust Inst* 2007;31:2247–55. doi:10.1016/j.proci.2006.07.111.
- [11] Zhu S, Roekaerts D, Meer T Van Der. Numerical study of a methanol spray flame. *Seventh Mediterr. Combust. Symp.*, 2011, p. 1–8.
- [12] Som S, Ramirez AI, Longman DE, Aggarwal SK. Effect of nozzle orifice geometry on spray, combustion, and emission characteristics under diesel engine conditions. *Fuel* 2011;90:1267–76. doi:10.1016/j.fuel.2010.10.048.
- [13] Shuai S, Abani N, Yoshikawa T, Reitz RD, Park SW. Evaluation of the effects of injection timing and rate-shape on diesel low temperature combustion using advanced CFD modeling. *Fuel* 2009;88:1235–44. doi:10.1016/j.fuel.2009.01.012.
- [14] Petranović Z, Vujanović M, Duić N. Towards a more sustainable transport sector by numerically simulating fuel spray and pollutant formation in diesel engines. *J Clean Prod* 2014. doi:10.1016/j.jclepro.2014.09.004.
- [15] Guo Y. A pure Eulerian model for simulating dilute spray combustion. *Fuel* 2002;81:2131–44. doi:10.1016/S0016-2361(02)00140-0.
- [16] Beck JC, Watkins AP. SIMULATION OF WATER AND OTHER NON-FUEL SPRAYS USING A NEW SPRAY MODEL. *At Sprays* 2003;13:1–26. doi:10.1615/AtomizSpr.v13.i1.10.
- [17] Dhuchakallaya I, Watkins AP. Application of spray combustion simulation in DI diesel engine. *Appl Energy* 2010;87:1427–32. doi:10.1016/j.apenergy.2009.08.029.
- [18] Xue Q, Battistoni M, Powell CF, Longman DE, Quan SP, Pomraning E, et al. An Eulerian CFD model and X-ray radiography for coupled nozzle flow and spray in internal combustion engines. *Int J Multiph Flow* 2015;70:77–88. doi:10.1016/j.ijmultiphaseflow.2014.11.012.
- [19] Bekdemir C, Somers LMT, de Goey LPH, Tillou J, Angelberger C. Predicting diesel combustion characteristics with Large-Eddy Simulations including tabulated chemical kinetics. *Proc Combust Inst* 2013;34:3067–74. doi:10.1016/j.proci.2012.06.160.
- [20] Boileau M, Pascaud S, Riber E, Cuenot B, Gicquel LYM, Poinot TJ, et al. Investigation of Two-Fluid Methods for Large Eddy Simulation of Spray Combustion in Gas Turbines. *Flow, Turbul Combust* 2007;80:291–321. doi:10.1007/s10494-007-9123-1.
- [21] Chrigui M, Gounder J, Sadiki A, Masri AR, Janicka J. Partially premixed reacting acetone spray using LES and FGM tabulated chemistry. *Combust Flame* 2012;159:2718–41. doi:10.1016/j.combustflame.2012.03.009.
- [22] Pickett L. European Combustion Network 2014. <http://www.sandia.gov/ecn/>.
- [23] Drew DA, Passman SL. *Theory of Multicomponent Fluids*. 1998.
- [24] FIRE manual 2013. Graz: 2013.
- [25] Reitz RD. Modeling atomization processes in high-pressure vaporizing sprays. *At Spray Technol* 1987;3:309–37.
- [26] O'Rourke PJ. Statistical properties and numerical implementation of a model for droplet dispersion in a turbulent gas. *J Comput Phys* 1989;83:345–60. doi:10.1016/0021-9991(89)90123-X.
- [27] Petranović Z, Edelbauer W, Vujanović M DN. The O'Rourke droplet collision model for the Euler–Eulerian framework. *Proc. 26th Conf. Liq. At. Spray Syst.*, 2014.

- [28] Vujanović M, Petranović Z, Edelbauer W, Baleta J, Duić N. Numerical modelling of diesel spray using the Eulerian multiphase approach. *Energy Convers Manag* 2015. doi:10.1016/j.enconman.2015.03.040.
- [29] Abramzon B, Sirignano WA. Droplet vaporization model for spray combustion calculations. *Int J Heat Mass Transf* 1989;32:1605–18. doi:10.1016/0017-9310(89)90043-4.
- [30] Robert J. Kee FMREMJAM. CHEMKIN-III: A Fortran Chemical Kinetics Package for the Analysis of Gas Phase Chemical and Plasma Kinetics," Sandia National Laboratories Report n.d.
- [31] Sarathy SM, Westbrook CK, Mehl M, Pitz WJ, Togbe C, Dagaut P, et al. Comprehensive chemical kinetic modeling of the oxidation of 2-methylalkanes from C7 to C20. *Combust Flame* 2011;158:2338–57. doi:10.1016/j.combustflame.2011.05.007.
- [32] Luo Z, Som S, Sarathy SM, Plomer M, Pitz WJ, Longman DE, et al. Development and validation of an n-dodecane skeletal mechanism for spray combustion applications. *Combust Theory Model* 2014;18:187–203. doi:10.1080/13647830.2013.872807.
- [33] Fuel/Engine Interactions n.d. <http://books.sae.org/r-409/> (accessed April 28, 2015).
- [34] Hanjalić K, Popovac M, Hadžiabdić M. A robust near-wall elliptic-relaxation eddy-viscosity turbulence model for CFD. *Int J Heat Fluid Flow* 2004;25:1047–51. doi:10.1016/j.ijheatfluidflow.2004.07.005.
- [35] Naber J, Siebers DL. Effects of Gas Density and Vaporization on Penetration and Dispersion of Diesel Sprays, 1996. doi:10.4271/960034.
- [36] Siebers DL. Scaling Liquid-Phase Fuel Penetration in Diesel Sprays Based on Mixing-Limited Vaporization, 1999. doi:10.4271/1999-01-0528.
- [37] Idicheria C a, Pickett LM. Quantitative Mixing Measurements in a Vaporizing Diesel Spray by Rayleigh Imaging. *SAE Int J Engines* 2007;01:776–90. doi:10.4271/2007-01-0647.
- [38] Pickett LM, Kook S, Williams TC. Visualization of Diesel Spray Penetration , Cool-Flame , Ignition , High- Temperature Combustion , and Soot Formation Using High-Speed Imaging. *SAE Int J Engines* 2009;2:439–59. doi:10.4271/2009-01-0658.
- [39] Pickett LM, Manin J, Genzale CL, Siebers DL, Musculus MPB, Idicheria C a. Relationship Between Diesel Fuel Spray Vapor Penetration/Dispersion and Local Fuel Mixture Fraction. *SAE Int J Engines* 2011;4:764–99. doi:10.4271/2011-01-0686.
- [40] Pickett LM, Genzale CL, Bruneaux G, Malbec L-M, Hermant L, Christiansen C, et al. Comparison of Diesel Spray Combustion in Different High-Temperature, High-Pressure Facilities. *SAE Int J Engines* 2010;3:156–81. doi:10.4271/2010-01-2106.
- [41] Pickett, L.M., Genzale, C.L., Manin, J., Malbec, L.-M. and Hermant L. Measurement Uncertainty of Liquid Penetration in Evaporating Diesel Sprays. ILASS-Americas, Ventura, California: 2011, p. Paper No. 2011–111.